Biophys Struct Mech (1983) 9: 145–170

Biophysics of Structure and Mechanism

Review

Structure and Function of Viroids

D. Riesner[1], G. Steger[1], J. Schumacher[1], H. J. Gross[2], J. W. Randles[3], and H. L. Sänger[4]

[1] Institut für Physikalische Biologie, Universität Düsseldorf, D-4000 Düsseldorf, Federal Republic of Germany
[2] Institut für Biochemie, Universität Würzburg, D-8700 Würzburg, Federal Republic of Germany
[3] Department of Plant Pathology, University of Adelaide, Waite Agricultural Research Institute, Glen Osmond, South Australia 5064
[4] Max-Planck-Institut für Biochemie, D-8033 Martinsried bei München, Federal Republic of Germany

Abstract. Viroids are an independent class of plant pathogens which are distinguished from viruses by the absence of a protein coat and by their unusually small size. They are single-stranded circular RNAs composed of about 360 nucleotide residues. Sequence analysis and physicochemical studies of the potato spindle tuber viroid (PSTV) have shown that, as a result of intra-molecular base pairing, viroids form a unique rod-like secondary structure which is characterized by a serial arrangement of double-helical sections and internal loops. There is no indication for an additional tertiary structure because all parts of the molecule are freely accessible to ligand interaction. During the denaturation all of the native base pairs of viroids are dissociated in one highly cooperative transition, and in the same process very stable hairpins which are not present in the native structure are newly formed. Most of the properties of the structure and structural transitions of PSTV have been found also in citrus exocortis viroid, chrysanthemum stunt viroid and four different viroid-like RNAs associated with the cadang-cadang disease. The close similarity between these viroids is more expressed in the overall structure and in thermodynamic and functional domains than in the primary sequence. The stiffness of all viroids can be described by an unique persistence length of 300 Å. Characteristically, regions of premelting, regions of stable hairpins, and the sequence UACUACCCGGUGG which is opposite to one of the stable hairpins, are the most conservative sequences in the molecules. Current hypotheses about the function of viroids are discussed on the basis of their structural and thermodynamic features. The suggestion that viroid RNA has features similar to DNA has been supported by the finding that they are replicated in vitro by the DNA-dependent RNA polymerase II of the host plant. The highly conserved sequence in viroids mentioned above corresponds very closely to a segment at the 5′-end of the small nuclear RNA U1 of eukaryotes. Because this segment is discussed in recent models, to be involved in the splicing process, a hypothesis is proposed in which viroids interfere with the splicing process leading to a pathogenic misregulation of mRNA processing.

Key words: Viroids – Thermodynamics – Kinetics – Hydrodynamics – Function

Content

I. Identification and Isolation

Viroids are the smallest infectious agents known. They are distinguished from viruses and bacteriophages by the absence of a protein coat and by their unusually small size. They were identified as a new and independent class of pathogens when different groups of researchers (T. O. Diener, USA, 1971; H. L. Sänger, Germany, 1972; J. Semancik, USA, 1972; R. P. Singh, Canada, 1971) found that diseases of certain higher plants were caused by short protein-free ribonucleic acids. Thus, viroids are single infectious molecules with a molecular weight around 120,000, i.e., a factor of 20 smaller than the smallest bacteriophages.

In spite of their small size viroids can be extremely pathogenic as shown in Fig. 1A, where a healthy and a viroid-infected tomato plant are depicted. Viroid diseases have been found with potato (Diener 1971), tomato (Singh 1972), citrusfruit (Sänger 1972; Semancik and Weathers 1972), chrysanthemum (Hollings and Stone 1973; Diener and Lawson 1973; Romaine and Horst 1975), cucumber plants (van Dorst and Peters 1974), coconut palms (Randles 1975), hops (Sasaki and Shikata 1977), avocado (Thomas and Mohamed 1979), and the ornamental plant *Columnea erythropae* (Owens et al. 1978). Probably the most economically important disease is cadang-cadang which has killed around 30 million coconut palms in the Philippinnes (Fig. 1B) (Zelasny et al. 1982). Viroids have not been found in man or animal although several diseases have been considered to be caused by viroid-like agents. Studies on viroids are not only of major importance in agriculture and horticulture but are also of basic

A

B

Fig. 1. Symptoms of viroid infections. In **A** a healthy tomato plant (left) and a plant infected with PSTV (right) is depicted. In **B** a grove of coconut palmes infected by the cadang-cadang disease in shown

interest in molecular biology. The coding capacity of viroids is apparently too small for them to direct the synthesis of enzymes reponsible for their own replication. Therefore, the structure, synthesis, and pathogenicity of viroids cannot be understood in terms of conventional viral mechanisms. Viroids are also of interest to biophysicists. They are of a size which is accessible to a series of physical techniques. They are one step more complex than the well known tRNA, but they are also markedly smaller than phage RNA. Besides tRNA, the structure of viroids is at present better understood than that of any other RNA.

A prerequisite of physical and physicochemical investigations was the availability of at least microgram amounts of highly purified viroid material. It was a long and tedious process to develop a procedure for isolating viroids from diseased plants (Sänger et al. 1976). Young tomato plants were found to be

appropriate for viroid propagation because they can be cultivated in large numbers in greenhouses and show clear symptoms a few weeks after viroid infection. Leaf material is homogenized, extracted with phenol, and the total nucleic acids remaining in the aqueous phase are precipitated with ethanol. Repeated precipitation and extraction steps are used to free the precipitate (which contains the infectious viroid RNA) from large nucleic acids and also from polysaccharides the presence of which complicates the purification considerably. Repeated preparative polyacrylamide gel electrophoresis finally yields a nucleic acid which is infectious, and which is absent from similar preparations derived from healthy plants. The yield of the purified viroid RNA is extremly low as only about 0.2 mg of pure viroid can be obtained from 5,000 diseased plants. Recently, HPLC-technique has been applied successfully for a large scale purification of viroids leading to a more simple and rapid isolation (Colpan et al. in preparation).

In this article we will describe the development of our present knowledge about the structure and dynamics of viroids and outline current concepts and hypotheses about their function. The article is centered mainly around the work of the authors with particular emphasis on the physical aspects of these studies. Biological and chemical features of viroids have been reviewed elsewhere (Diener 1979; Gross and Riesner 1980; Sänger 1981; Kleinschmidt et al. 1981).

II. Structure

Following purification of viroids in sufficient quantity early studies centred on their structure. Details of their structure could then be used as a basis for present and future studies on their function.

Only those techniques which can be applied to microgram amounts of viroid RNA could be used for structural studies. For example, very small amounts of RNA are needed for electron microscopy. Furthermore the modern techniques of nucleotide sequencing require little material because the nucleic acid or its fragments are radioactively labeled in vitro and detectable in subsequent steps by autoradiography methods. Physicochemical methods can also be refined for small and low concentration samples if they take advantage of the high UV-absorption coefficients of nucleic acids. Therefore, thermodynamic, kinetic, and hydrodynamic studies with UV-recording can be done systematically whereas calorimetry, NMR etc. can be applied only when sufficient quantities are available.

1) Electronmicroscopy

Under native conditions viroids appear in electronmicrographs as rod-like molecules of an average length of 37 ± 6 nm (Fig. 2A) (Sänger et al. 1976; Riesner et al. 1979). The shape of viroids has also been studied with hydrodynamic methods in solution. By determining the molecular weight and

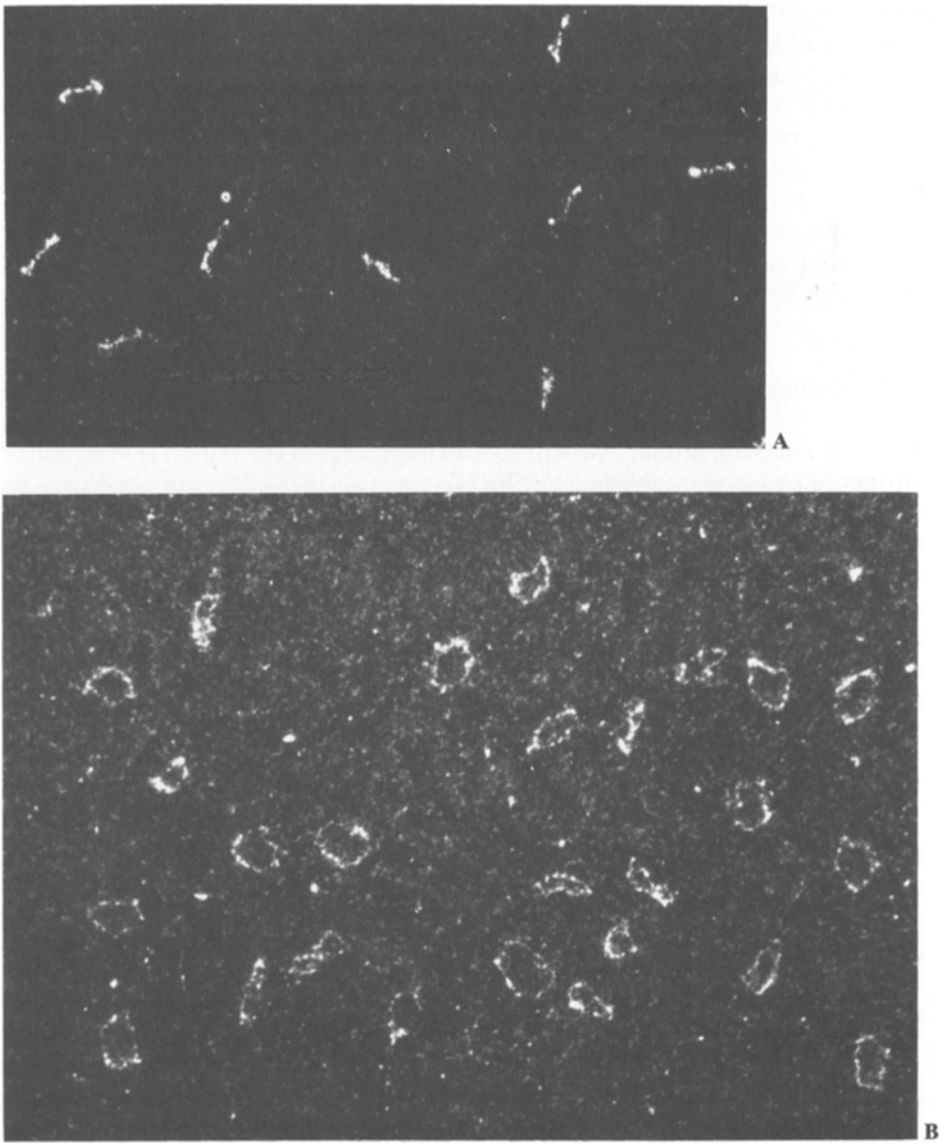

Fig. 2. Electromicrographs in dark-field illumination of viroids in the native conformation (**A**) and as relaxed circles (**B**). Magnification is 185,000

sedimentation coefficient independently, an axial ratio of 20 : 1 has been estimated – a value in good agreement with the results from electronmicroscopy.

Spreading and grid preparation was also carried out under fully denaturing conditions (see below), i.e., after all basepairs are disrupted by urea, by formamide or by elevated temperatures, and the resulting structures were

sometimes fixed with formaldehyde. Viroids are then visible as covalently closed single-stranded circles with a contour length of 100 ± 6 nm (Fig. 2B) (Sänger et al. 1976; McClements and Kaesberg 1977; Riesner et al. 1979). This conclusion was clearly confirmed by chemical methods (see below). The discovery that viroids were circular was surprising and viroids were the first example of a natural circular RNA. Ring structures had previously only been found in DNA, and these were of much higher molecular weight. In the mean time circular RNA molecules of various size have recently also been found in the cytoplasm and in mitochondria of eukaryotic cells (Ming-Ta Hsu and Coca-Prados 1979; Arnberg et al. 1980).

2) Nucleotide Sequence of PSTV

The first complete primary structure of a viroid, that of the potato spindle tuber viroid (PSTV), was established in 1978 (Gross et al. 1978). We will not discuss in this context the particular difficulties which made the work on the sequence of the 359 nucleotides of PSTV a very difficult task, we will take the result of that work as a basis for further quantitative treatments. While discussing structural aspects it should be pointed out that distribution of enzyme digested fragments in PSTV showed unequivocally that the 359 nucleotides of PSTV form a covalently closed circle. The nucleotide sequence and the secondary structure sequence of PSTV are shown in Fig. 3.

3) Thermal Denaturation and Secondary Structure of Viroids

In the viroid circle, the formation of intramolecular basepairs leads to a well defined secondary structure. This structure can be derived either from the nucleotide sequence by calculating the thermodynamically most stable structure or from thermodynamic experiments.

Calculation of the Most Stable Structure. The stability constants, the reaction enthalpies and entropies for basepair formation are given in the literature (Borer et al. 1974; Gralla and Crothers 1973a, b; Pörschke et al. 1973; Rubin and Kallenbach 1975; Scheffler et al. 1970; Riesner et al. 1979; Steger et al. in preparation). Firstly they depend on the type of the basepair formed and the type of the neighboring basepair. In addition to the classical Watson-Crick basepairs, A : U and G : C, the so called wobble type G : U is also taken into account. Furthermore, if a basepair is formed as a first pair closing a loop the parameters depend upon the size and kind of the loop. In Table 1 the different elementary steps for secondary structure formation are listed. Several graphical and computerized methods are available to search for highly basepaired structures of a given sequence. The highly basepaired structure is considered to arise from the unpaired circle as the product of a multistage process of the elementary steps whose contribution to the overall free energy are then summed. The basepairing scheme with the lowest free energy is the

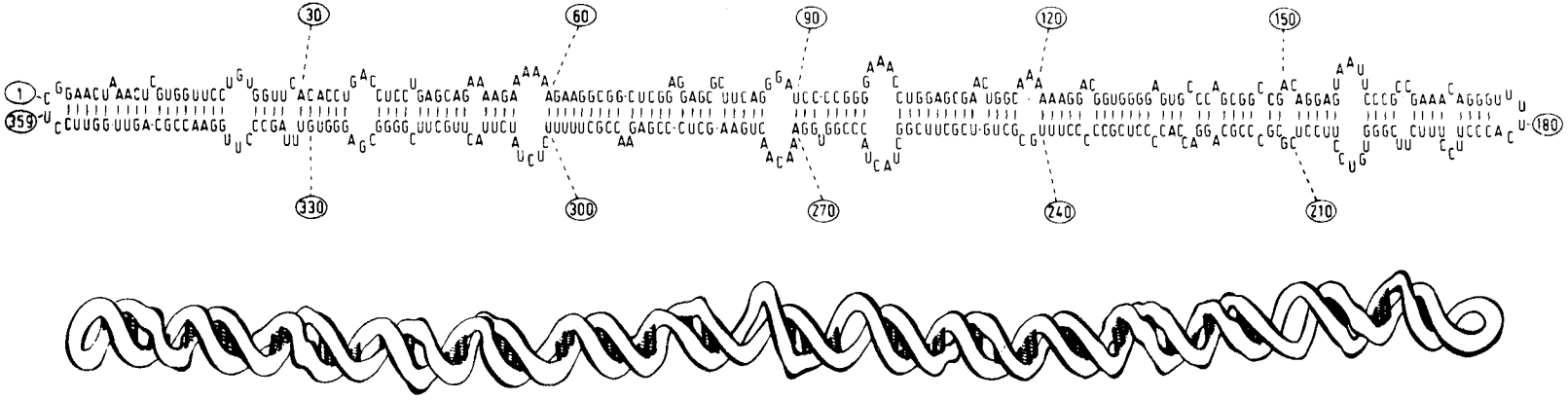

Fig. 3. Structure of PSTV. Basepairing sheme (top), three dimensional representation (bottom)

Table 1. Stability parameters of ribonucleic acids. The values for the equilibrium constants, reaction enthalpies, and reaction entropies can be found in the literature (see text). The growth parameters of base pairing (see 1) not only depend upon the type of base pair to be formed but also upon the type of the preceding base pair. Loop formation (see 2) depends upon the factor γ, which describes the probability of pairing of bases which are within a favorable distance, and upon the loop weighting function $\varrho\ (p+1)$ which describes the probability of approaching the favorable distance and includes the geometry of the loop. l_{tot} = total number of nucleotides of the molecule

1) Base pairing $s_{\substack{G\\C}}^{\substack{G\\C}}$, $s_{\substack{A\\U}}^{\substack{G\\C}}$, $s_{\substack{A\\U}}^{\substack{A\\U}}$:Experimental	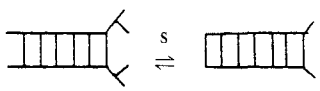
2) Loop formation A) Hairpin loop $p < 13$: Experimental Monte-Carlo-calculations $p \geqq 13$: $\varrho\ (p+1) = 0.319 \cdot p^{\frac{3}{2}}$	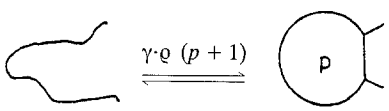
B) Internal loop $r \leqq 8$: Experimental $r > 8$: $\varrho_i = \varrho\ (r+1)$	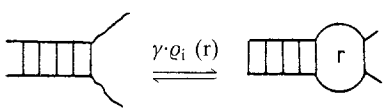
C) Bulge loop $t \leqq 8$: Experimental $t > 8$: $\varrho_b\ (t) = \varrho\ (t+1)$	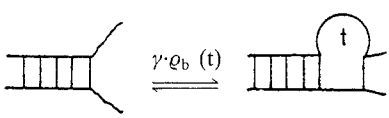
3) Base pairing in circles $K = \gamma \frac{\varrho(p+1) \cdot \varrho\ (q+1)}{\varrho(l_{tot})} \cdot S^{N-1}$	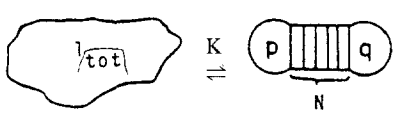

thermodynamically most favorable secondary structure. This structure is shown for PSTV in Fig. 3 (Riesner et al. 1979). A similar scheme is obtained as a first order approximation if the number of basepairs is optimized (Gross et al. 1978).

Secondary Structure as Concluded from Melting Curves. The helix-coil transition of nucleic acids can be induced by temperature increase, and it is associated with a 30–40% increase in UV-absorption. These transition curves, commonly called melting curves, can nowadays be recorded with computer controlled spectrophotometers, using microcuvettes of 50 µl sample volume and 1 cm optical pathlength. Consequently, less then a microgram of nucleic acid is needed to obtain a melting curve (Henco et al. 1980). In Fig. 4 melting curves of PSTV and

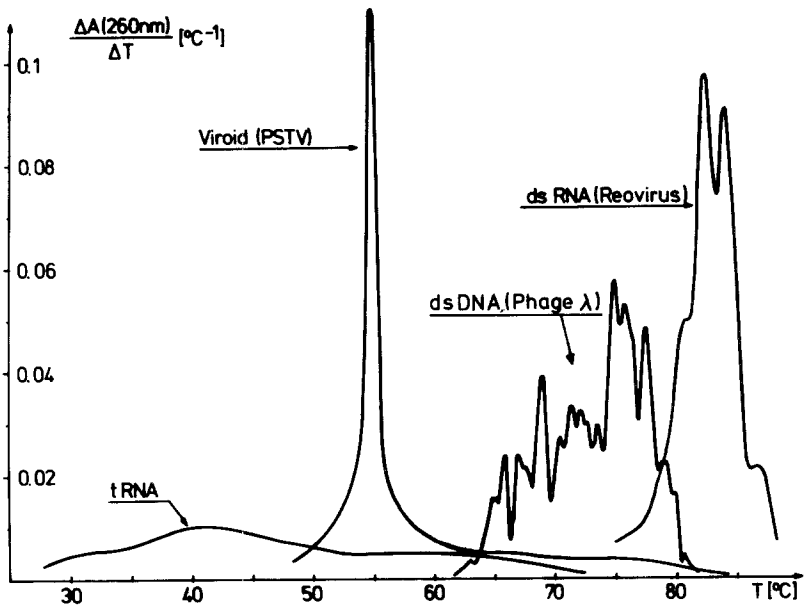

Fig. 4. Optical denaturation curves of PSTV, $tRNA^{Phe}$ from yeast, dsRNA from reovirus and dsDNA from phage λ. The curves are presented in the differentiated form. Buffer conditions: 1 mM sodium-cacodylate, 20 mM NaCl, pH 6.8, 0.1 mM EDTA; concentration of the nucleic acid: A_{260} (20° C) = 1

other types of RNA and DNA are depicted. Melting curves in the differentiated form as in Fig. 4 are commonly used today because the occurence of more than a single transition can be recognized more easily and the evaluation of the midpoint temperature T_m and the half width $\Delta T_{1/2}$ is easier (Riesner and Römer 1973).

It is quite obvious from Fig. 4 that different nucleic acids can give rise to quite different melting curves. tRNA shows the well known curve of several broad transitions at a fairly low average T_m-value. The other extreme is the denaturation of homogenous double-stranded RNA from reovirus, which occurs in several very sharp transitions at high temperatures. DNA from phage λ shows a multistep curve at somewhat lower temperatures than the reovirus RNA. An extraordinary situation is found with PSTV in that the sharpness of the transition of a double-stranded nucleic acid is combined with the low thermal stability of single-stranded nucleic acids such as tRNA, 5SRNA and mRNA.

Before the complete sequence of PSTV was known some essential features of its secondary structure could be derived from the transition curves (Langowski et al. 1978). Secondary structural models of viroids were varied systematically, the corresponding melting curves were calculated applying known methods of statistical thermodynamics, and the simulated melting curves were compared with the experimental ones. Best agreement was obtained for a secondary structure model in which short double helices and small internal loops are arranged in an unbranched series. This model agreed with great accuracy with the detailed secondary structure derived from the nucleotide sequence.

Now that the sequences of several viroid species are known, it is of course more appropriate to discuss the structural and dynamic details of viroids on the basis of their established sequences.

So far, the results from thermodynamic studies have been interpreted in terms of the structures involved, whereas the real mechanistic properties will be discussed together with the kinetic results in the next section. We wish, however, to emphasize one qualitative argument. As mentioned before, viroids combine the sharpness of the transition, i.e., the cooperativity, of double-stranded nucleic acid with the low T_m of single-stranded, clover-leaf like RNA structures. Indeed, both structural features are found in viroids. As has been shown quantitatively, the complete linear arangement in combination with the circularity serves for the maintainance of the cooperativity, and the many internal loops decrease the melting temperature.

4) Absence of an Additional Tertiary Structure

It is known from other single-stranded RNAs such as tRNA, 5SRNA, ribosomal RNA etc. that in addition to the two dimensional secondary structure a higher ordered structure may be formed which is termed the tertiary structure. The L-shaped tRNA is the best studied example of a nucleic acid with pronounced tertiary structure. At first glance, viroids with the many unpaired regions would appear to be predestinated to bend to a more globular structure and form additional basepairs between loops which are quite distant in the secondary structure. Results from different experiments have proven, that the extended form as suggested from the secondary structure and visualized at the bottom of Fig. 3 is actually present in solution (Gross and Riesner 1980). Besides the electronmicroscopic and the hydrodynamic studies already mentioned, studies with dye binding to the helical regions (Riesner et al. 1979), oligonucleotide binding to the unpaired regions (Wild et al. 1980), enzymatic digestion in the loops (Gross et al. 1978), and chemical modification of unpaired cytosines (Gross et al. 1978), have shown quantitative agreement with a molecular structure in which all tested regions are freely accessible. The rigidity or stiffness of the rod-like structure will be discussed below.

III. Structural Transitions

Whereas in the last section structural aspects were dominant in interpreting the thermal denaturation of viroids, we turn now to more mechanistic questions. A close inspection of the melting curve of PSTV in Fig. 4 shows that after the main transition has occurred broader transitions of lower hypochromicity are found at higher temperatures. Because of the low signal these transitions were not resolvable by equilibrium melting. In the temperature-jump technique, however, a denaturation process is characterized not only by its overall hypochromicity but also by its complete, exponential time course after a stepwise temperature increase or decrease. If more than one process contributes, more than one exponential with a corresponding amplitude is measurable. The slow temperature-jump technique in which the temperature

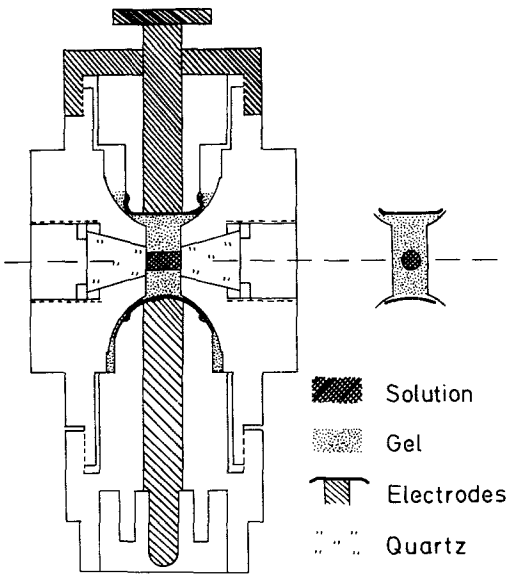

Fig. 5. Vertical cross section through the microcell for the temperature-jump-technique. On the right the front view of the compartment containing the gel and the sample is shown. The dashed line represents the axis of the light beam. The body of the cell was made from Delrin (Du Pont). When the cell was used in the conventional manner, it was filled only with solution instead of gel and solution, and 1.2 ml sample had to be used instead of 80 µl

change is induced by switching thermostating bathes, as well as the fast technique with temperature-jumps resulting from capacitor discharge were applied to cover the time range from microseconds to minutes (Henco et al. 1979). Both techniques were optimized for the requirements of the study on viroids, i.e., high temperatures and exceedingly little RNA material (Henco et al. 1980; Riesner et al. 1982a). An essential improvement was developed for the cell of the discharge T-jumps in which the sample volume was reduced from 1.2 ml to 80 µl without changing the optical pathlength or the thermal properties. As illustrated in Fig. 5, an agarose gel was formed between the electrodes and the sample was placed in a hole of small bore cut from one window to the other.

1) Main Transition

The kinetic results confirmed the high cooperativity of the main transition. 80–90% of the hypochromicity is found in a single exponential relaxation effect in the time range of seconds. If the cooperativity is determined by a comprison of reaction enthalpy evaluated from van't Hoff plots and the total enthalpy measured calorimetrically, a ratio $\Delta H_{\text{van't Hoff}}/\Delta H_{\text{total}} = 0.8-0.9$ was obtained. In Fig. 6A the amplitudes and relaxation times of the highly cooperative process are given, and in Table 2 some parameters which were derived from the equilibrium and kinetic investigations are listed (Henco et al. 1979).

2) Transition at Higher Temperatures

Although the amplitudes amounted to only a few percent of those of the main transition the processes could be followed quantitatively by fast kinetic

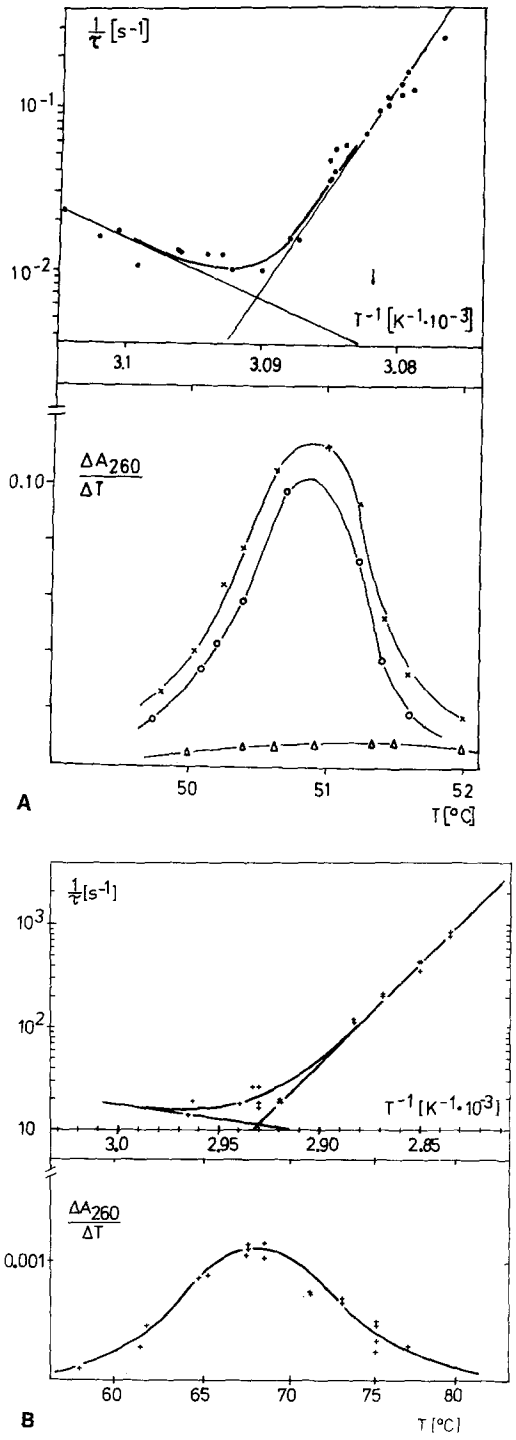

Fig. 6. Temperature dependence of the relaxation times (upper graphs) and the hypochromicity (lower graphs) measured in the main transition (**A**) and in the high temperature transition (**B**). The relaxation times τ are presented in form of Arrhenius plots log $1/\tau$ vs. 1/T. The hypochromicities are taken from the relaxation amplitudes. In **A** the contributions of the process in the s-range (○) and in the ms-range (△) to the total hypochromicity (×) are shown

Table 2. Properties of the main transition. The numbers of basepairs given in parentheses correspond to the structures in Figs. 3 and 8. Because a few basepairs dissociate at very low temperatures, the numbers of basepairs taking part in the main transition (without parentheses) are lower. T_m-values correspond to 1 mM Na-cacodylate, 10 mM NaCl, 0.1 mM EDTA, pH 6.8. Cooperativity is defined as the ratio (given in %) of $\Delta H_{van't\ Hoff}$ to the ΔH-value which was expected if all basepairs involved in the main transition would dissociate in a completely cooperative manner. No values of the cooperativity can be given for ccRNA2 because two transitions are involved

	Number of nucleotides	Basepairs of the native structure	T_m (°C)	Hypochromicity (%)	f_{GC} (%)	$\Delta H_{van't\ Hoff}$	Cooperativity (%)
PSTV	359	121 (124)	51.0	14	66 ± 2	3,885 ± 240	88 ± 4
CEV	371	123	51.0	14	65 ± 2	3,490 ± 200	73 ± 4
CSV	354	116 (120)	48.5	18	59 ± 3	3,130 ± 150	72 ± 3
ccRNA1							
Small	246/7	72 (77)	49.1	15	70.0 ± 1	2,470 ± 100	86 ± 3
Large	295 (±8)	89 (94)	49.4	16.5	72.5 ± 1	2,880 ± 130	81 ± 3
ccRNA2							
Small	482/4	146 (156)	46.7	12	73.0 ± 1		
Large	590 (±16)	180 (190)	47.1	14.5	74.0 ± 1		

measurements (Henco et al. 1979). In Fig. 6B the relaxation amplitudes and times are given for the transition with the highest T_m-value in PSTV. Those data, together with the wavelength dependence of the hypochromicity $Hy(\lambda)$ led to a complete set of parameters which allowed us to attribute the process to a well defined region in the viroid molecule. Briefly, it was carried out as follows: $Hy(\lambda)$ yielded the G : C content, ΔH together which the G : C content the number of basepairs, k_R allowed the estimation of the number of unpaired bases in the loop which is closed by formation of the first basepair. The consistency of these data may checked by the T_m-value. Then, a search was made for particularly stable complementary regions in the viroid sequence which could form hairpins. In Table 3 the hairpins which have been found in PSTV and in other viroids (see below, Henco et al. 1979; Randles et al. 1982), are listed, and the experimentally determined parameters (exp) are compared with those calculated (the) on the basis of the sequences. We regard the agreement as experimental proof of the presence of those hairpins at temperatures above the main transition.

An unexpected result is that the stable hairpins are not part of the native structure but have to be newly formed during the main transition. Consequently, all basepairs of the native structure are disrupted in the main transition and particularly stable double-helices between regions quite distant in the native structure are newly formed.

3) Complete Denaturation Scheme

After identifying the stable hairpins the complete mechanism of denaturation and renaturation is as illustrated in Fig. 7. In the main transition the extended native structure (a in Fig. 7) switches over into a branched structure (c in Fig. 7). In PSTV three stable hairpins would follow from the sequence, whereas from the experiments the presence of only two of them can be concluded safely. In the two consecutive steps the stable hairpins dissociate into the completely unpaired circle. All structural states could be observed in the electronmicroscope under the appropriate conditions of preparation (Riesner et al. 1979).

The formation of the stable hairpin increases the cooperativity of the main transition. For an easier explanation of this effect a transient state (b) which is not present in measurable concentrations is also depicted. It can be calculated that the left part of PSTV (helix 1–13 from left to right) would melt a few degrees lower than the right half. In the dissociated left half, however, sequences of nucleotides become unpaired and these can form the stable hairpins described above if they combine with their complementary sequences which are still involved in the native structure of the right half of the molecule. The strong tendency to form the stable hairpins (cf. the arrows in Fig. 7b) is inevitably a strong driving force for the dissociation of the right half of the molecule. It was calculated that the T_m-value of the right half is lowered thereby, and left and right halves dissociate at the same temperature.

Table 3. Properties of the stable hairpins. The theoretical values (the) are calculated from the sequences and the base pairing schemes. T_m-values correspond to 1 M ionic strength. The experimental values (exp) were evaluated from temperature-jump experiments. The experimental T_m-values were extrapolated to 1 M ionic strength assuming $dT_m/d \log C_{Na+} = 12.5°$ C. The numbers of basepairs were evaluated from the reaction enthalpies. Hairpin I is also present in CEV and CSV but was not followed quantitatively

Hairpin	T_m (°C)		f_{GC} (%)		Loop size		Number of basepairs	
	the	exp	the	exp	the	exp	the	exp
PSTV								
79 87 ~C G C U U C A G G I ⑭ ~G C G A G G U C C 110 102	86		69		14		9	
		80–85		77±5		20±10		>6[a]
127 133 ~C G G U G G G G A (III) ㉘ ~G C C G C C C U U 168 162	>86		85		28		7	
227 236 ~C C C U C G C C C C II ㉜ ~G G G A G C G G G G 328 319	92	93	90	90±5	82	>40	10	10±1
CEV								
239 249 C C C U C G C C C G G A G II ㊴ G G G A G C G G G C C U C 339 329	98	95	91	90±5	79	>40	11	10±1
CSV								
223 234 ~C C C U A G C C C G G II ㊱ ~G G G A U C G G G C C 322 311	92	97	82	95±5	76	>40	11	9±1
ccRNA1 large								
42 50 ~C G C U U G A G G I ⑭ ~G C G A A C U C C 73 65	85	87	67	71±7	14	20±10	9	10±1

[a] Because of the superimposition of both transitions only a lower limit could be evaluated

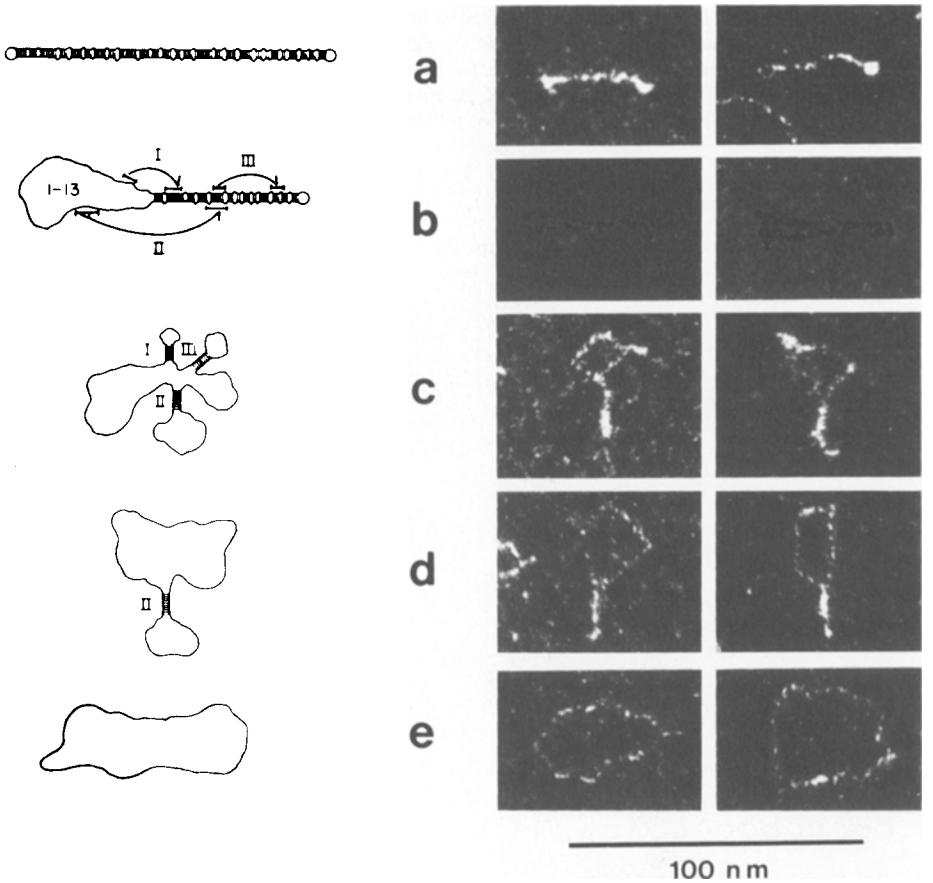

Fig. 7. Denaturation mechanism of PSTV. The molecule undergoes the transitions from (**a**) to (**e**) with increasing temperature. On the right side electron micrographs of PSTV in the corresponding conformations are shown (courtesy of Dr. G. Klotz, Ulm). Because conformation (**b**) is a kinetic intermediate, it is not observable in electron micrographs

IV. Viroids: A Structural and Dynamic Principle

Hydrodynamic, thermodynamic and kinetic studies have given a clear indication that other viroid species exhibit features very similar to PSTV (Sänger et al. 1976; Langowski et al. 1978). More specific comparison can be done now that more sequences are known. Figure 8 shows the sequences in the optimized secondary structures of citrus exocortis viroid (CEV; Gross et al. 1981, 1982), chrysanthemum stunt viroid (CSV; Gross et al. 1981, 1982; Haseloff and Symons 1981), and the viroid RNAs associated with the cadang-cadang-disease (ccRNA; Mohamed et al. 1981; Haseloff et al. 1982). As evident from Fig. 8 cadang-cadang disease differs from other viroid diseases in that four RNAs of different size which are, however, closely related each other, are associated with the disease (Imperial et al. 1981). The sequence homology between PSTV, CEV

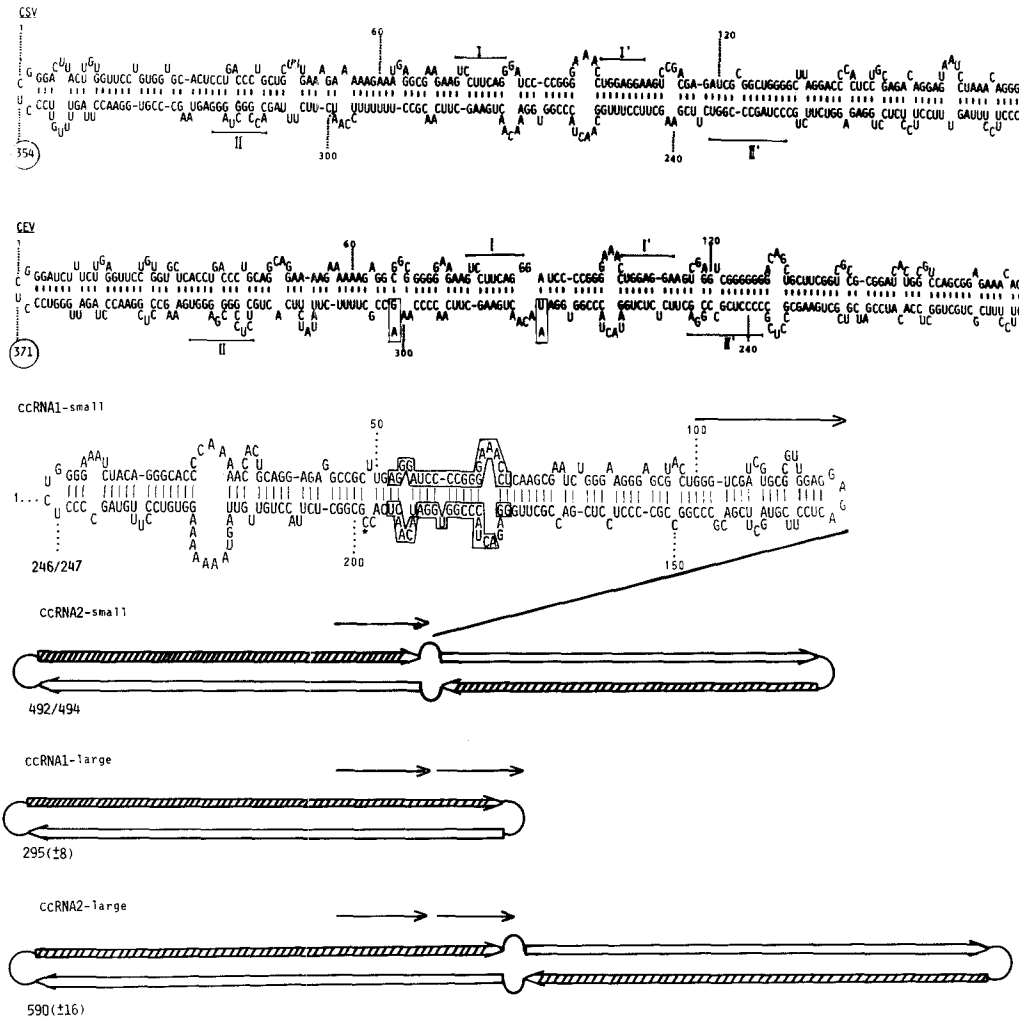

Fig. 8. Sequences and secondary structures of CEV, CSV and the four cadang-cadang-RNAs. Cadang-cadang RNA-small is a mixture of the sequence depicted and the sequence with C(198) missing. Cadang-cadang RNA-large differs from cadang-cadang RNA-small by duplication of the region marked by an arrow. The size of the duplicated region varies between different isolates leading also to a variation in the total number of nucleotides. RNA 2 is the duplication of RNA1 as depicted schematically. The boxed in region is identical in all viroids of this figure and PSTV. The sequences of CEV and CSV are those given by Gross et al. (1982), the sequences of ccRNA are taken from Haseloff et al. (1982)

and CSV is 60–70%, whereas ccRNA contains only in the boxed region a sequence conserved in all viroids. The properties of PSTV will be briefly reviewed with a discussion of their applicability to the other viroids.

1) Linear Arrangements of Short Double Helices and Small Internal Loops

As evident from Fig. 8 all viroids studied show a common principle in their secondary structure. Although the degree of basepairing is similar, the detailed

distribution of internal loops varies. Thus, in viroids the specific features of the secondary structure are evidently more conservative than the primary sequences. This result would not be expected a priori because only particular sequences are able to produce such a high degree of basepairing. It has been shown that randomly generated sequences with the same A : U : G : C ratio as PSTV would lead to only about 100 instead of 125 basepairs being formed (Riesner et al. 1979).

2) Premelting Regions and the Border of Stability

The optimal secondary structures have also been calculated at a temperature three degrees below the main transition. At this temperature the regions of lowest stability undergo premelting transitions. The premelting regions have been compared for CEV, CSV and PSTV, the viroids of high sequence homology (Gross et al. 1981; Steger et al. in preparation). In Fig. 9 two premelting regions show up in each of the three viroids. For an easier comparison, conservative and variable nucleotides are marked by different symbols. Thus, it is evident that the premelting regions are in conserved parts of the molecule. The left premelting region contains the oligo A sequence which was suspected to act as a promotor in viroid replication – without any experimental proof so far. The second premelting region is directly adjacent to one of the most stable helices. This borderline in the thermal stability is conserved in all of the three viroids in the form of a longer stretch of identical sequences. It divides the molecule in a less stable left half and a more stable right half. Looking at viroids from the point of molecular evolution one may see that the left part of viroids had been selected for particular sequences embedded in a structure which dissociates more easily compared to the right part; the right appears to have evolved toward a stable secondary structure with significantly less sequence conservation.

3) Cooperativity and Stable Hairpins

In the sequence of PSTV, CEV and CSV two stable hairpins – in PSTV possibly three – can form and these have been observed experimentally (Henco et al. 1979). Their cooperativity, T_m-values and the whole denaturation mechanism are very similar (cf. Tables 2 and 3) although species-specific differences are measurable and will be interpreted quantitatively on the basis of the sequences in a forthcoming paper (Steger et al. in preparation).

In general, the cadang-cadang RNAs fit into the picture outlined above (Randles et al. 1982). As shown in Fig. 10A, the main transition in ccRNA1 is as cooperative as in the other viroids. At higher temperatures an additional transition which was also studied by the kinetic technique (cf. Table 3), is detectable in the equilibrium melting and correlates to hairpin I in the other viroids. This transition is well resolved because the more stable hairpin whose melting is superimposed in the other viroids is absent in ccRNA. Therefore,

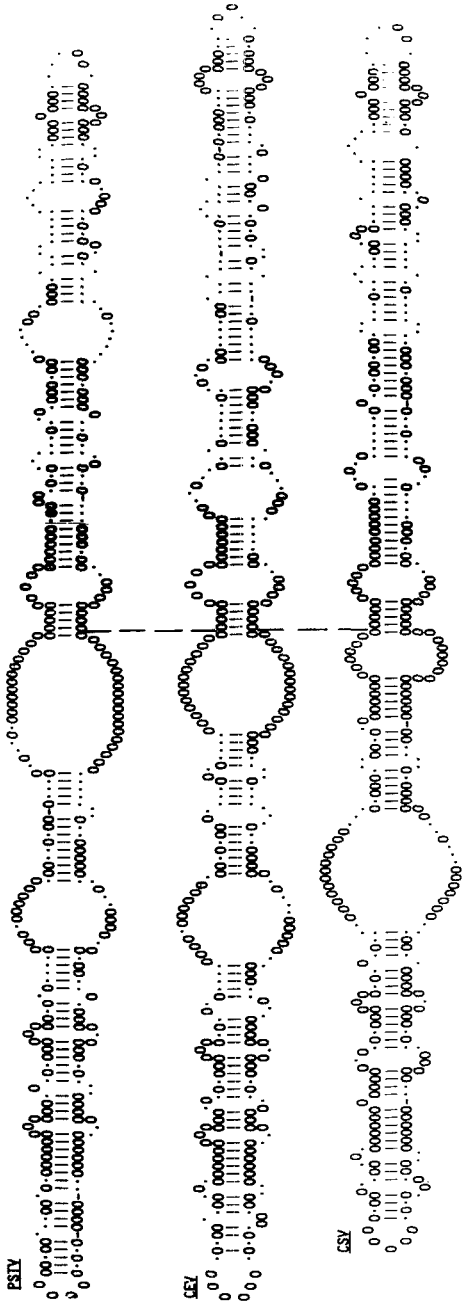

Fig. 9. Secondary structure of PSTV, CEV, and CSV at a temperature 3° C below the main transition. Nucleotides which are identical in the three viroids are represented by open circles, varying nucleotides by points. The dashed line represents the border of stability (see text)

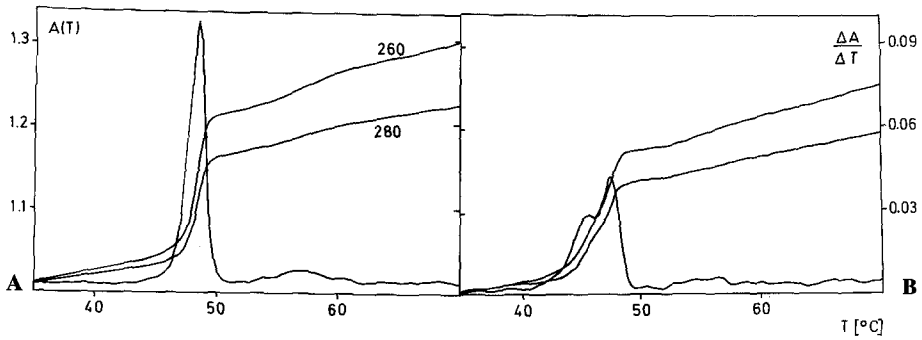

Fig. 10. Denaturation curve of cadang-cadang RNA1 (**A**) and a mixture of RNA1 and RNA2 (**B**). In addition to the differentiated curve at 260 nm $\Delta A/\Delta T$, the total absorbances at 260 nm and 280 nm which were measured simultaneously, are given

hairpin I appears to be a common property of viroids and, as will be discussed below, is probably of basic functional importance.

The size of PSTV, CEV and CSV seems to be the maximum for a viroid-type structure in which a highly cooperative transition is possible. For example, in ccRNA2, which is an exact duplication of ccRNA1, the high cooperativity is not maintained (Randles et al. 1982). The corresponding melting curve in Fig. 10B, shows that the main transition is 2.5° C lower and nearly twice as wide as that of ccRNA1. A detailed discussion of both molecules, and particularly the site of duplication, might explain the loss in cooperativity.

4) Hydrodynamic Model of a Worm-Like Structure with a Unique Persistence Length

The structural models discussed so far have been static models, and dynamic aspects of the structure have been determined from the thermodynamic and kinetic properties of the transitions from the native to the denatured states. Here we discuss aspects of the conformation of the native viroid, such as their structural flexibility or "stiffness".

Current theories about the stiffness of "worm-like" chain polymers allow the hydrodynamic behaviour of those polymers to be calculated (De la Torre and Bloomfield 1981). If a series of homologous polymers is studied, the dependence of the hydrodynamic properties upon contour length and molecular weight may be considered. The application of these theoretical treatments became possible only when viroids or viroid-like RNAs of different molecular weight were available for physico-chemical studies. At present, viroids from 246 nucleotides (ccRNA1-small) up to 600 nucleotides (ccRNA2-large) are available. The sedimentation coefficients of all viroids have been measured in the analytical ultracentrifuge and have been compared to those of dsDNA and dsRNA as shown in Fig. 11 (Riesner et al. 1982b). A plot of s versus log M was chosen because rigid-rod structures exhibit a linear dependence in this plot and deviation from the linear behaviour can be interpreted as coming from

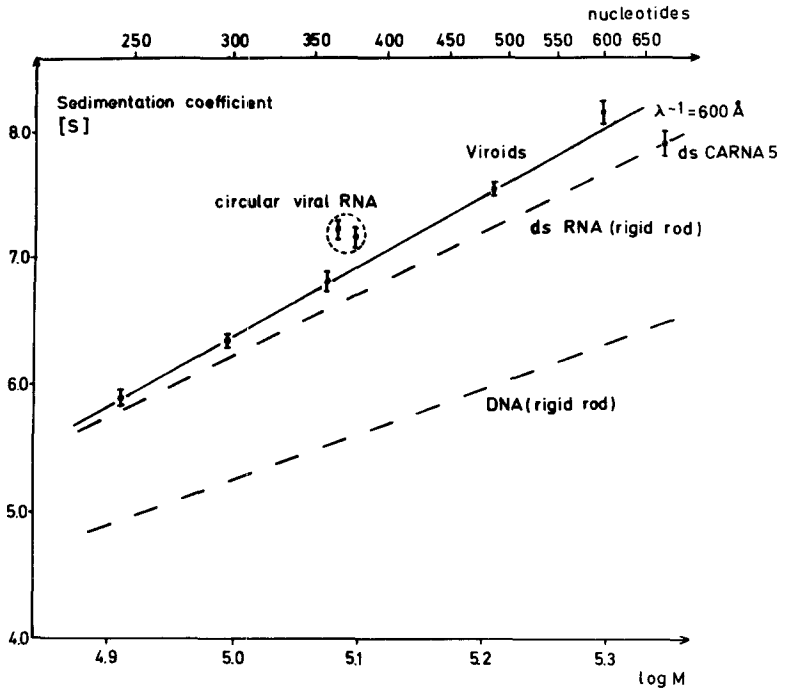

Fig. 11. Dependence of the sedimentation coefficients upon the logorithm of the molecular weight. The dashed line for double-stranded DNA is taken from the literature (Kovacic and van Holde 1977). The dashed line for double-stranded RNA was calculated for the RNA-11-helix assuming a hydrated diameter of 29 Å in accordance with the experimental s-value of double-stranded RNA5 associated with the cucumber mosaic virus (dsCARNA5). The fit to the s-values of viroids is calculated assuming a Kuhn's statistical length λ^{-1} of 600 Å. λ^{-1} of 600 Å corresponses to a persistence length of 300 Å. Circular viral RNAs are from Velvet tobacco mottle virus and *Solanum nodiflorum* mottle virus

measurable flexibility. Applying the calculus of Yamakawa and Fujii (1973), the s-values of viroids fit a line with a unique persistence length of 300 Å. This means that the largest viroid can bend in solution to more than a quarter of a circle. The unique persistence length of viroids seems to be a viroid specific property, because circular viral RNAs from velvet tobacco mottle virus and *Solanum nodiflorum* mottle virus which form a viroid-like secondary structure are clearly distinct from viroids in their hydrodynamic behaviour (Randles et al. 1981; Haseloff and Symons 1982). It is seen from Fig. 11 that they are markedly more flexible than viroids.

In summary, the viroids studied form a class of RNA molecules with very homogeneous features concerning structure, structural transitions and hydrodynamic behaviour. Recently, Symons (1981) reported the sequence and some other properties of the avocado sun blotch viroid (ASBV). This viroid also forms the characteristic secondary structure, but is different in stability and cooperativity from the other viroids. Symons argued that ASBV may belong to another class of viroids which have evolved separately from the other viroids studied so far.

V. Functional Hypotheses

This review emphasizes the structure and dynamics of viroids, and the possible functional role of the physical properties already described on viroid replication and pathogenesis is now discussed. There are three conspicous features which first led to speculation on the importance of structure and function. These are the circularity, the secondary structure of the linear arrangement of helices and loops, and the ability to form stable hairpins.

1) DNA-Likeness and Replication

It has been suggested at an earlier stage of the structural investigations that viroids posses features which are more characteristic of double-stranded DNA then of single-stranded RNA (Riesner et al. 1979). As visualized in Fig. 3, the overall shape of a viroid is similar to pieces of double-stranded nucleic acid. The circularity and the sesondary structure lead to highly cooperative transitions occuring at relatively low temperature. This high cooperativity is normally found with double-strands, not with single-strands, and the low T_m-value is closer to that of a double-stranded DNA than that of a double-stranded RNA (cf. Fig. 4). The hydrodynamic behaviour of viroids can be described quantitatively from their persistence length of 300 Å. If this number is compared to the 600 Å persistence length of homogeneous double-stranded DNA (Kovacic and van Holde 1977), one has to conclude that the many loops in viroids only gradually decrease the stiffness but do not lead to a different type of hydrodynamic model.

This early speculation has recently been supported by the evidence that viroids may be replicated in vitro to full length copies by the DNA-dependent RNA polymerase II (Rackwitz et al. 1981). This enzyme, found in healthy viroid host plants transcribes precursors of mRNA from the double-stranded DNA-genome. The in vitro mechanism cannot be said to apply to the in vivo situation but it supports the possibility that viroids are replicated in the host because they have features similar to DNA.

2) Stable Hairpins and Splicing Interference

Another remarkable property of all viroids (except ASBV, see above) is their ability to form the stable hairpin I (cf. Table 3) which is located in a highly conserved sequence. The segment which is located in the secondary structure opposite to that hairpin is also highly conserved. Even more remarkable is the close agreement of this sequence with the sequence at the 5′-end of U1RNA, a small nuclear RNA from eukaryotes. According to recent models, U1RNA is involved in the splicing process in which the so called introns are cut out from the heteronuclear RNA, and the processed mRNA, the exon, is formed. In these models the 5′-end of U1RNA forms basepairs with both ends of the intron (Fig. 12 according to Lerner et al. 1980). Thus, a particular arrangement of the

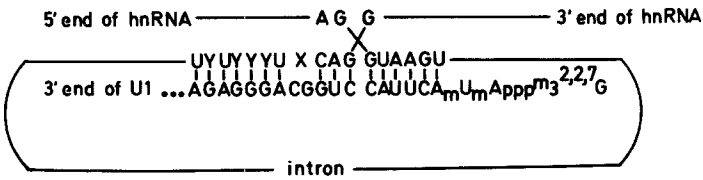

Fig. 12. Model of the involvement of U1RNA in the splicing process of heteronuclear RNA. The 5'-end of U1RNA forms a partially base paired region with the intron sequences next to the splicing site (according to Lerner et al. 1980)

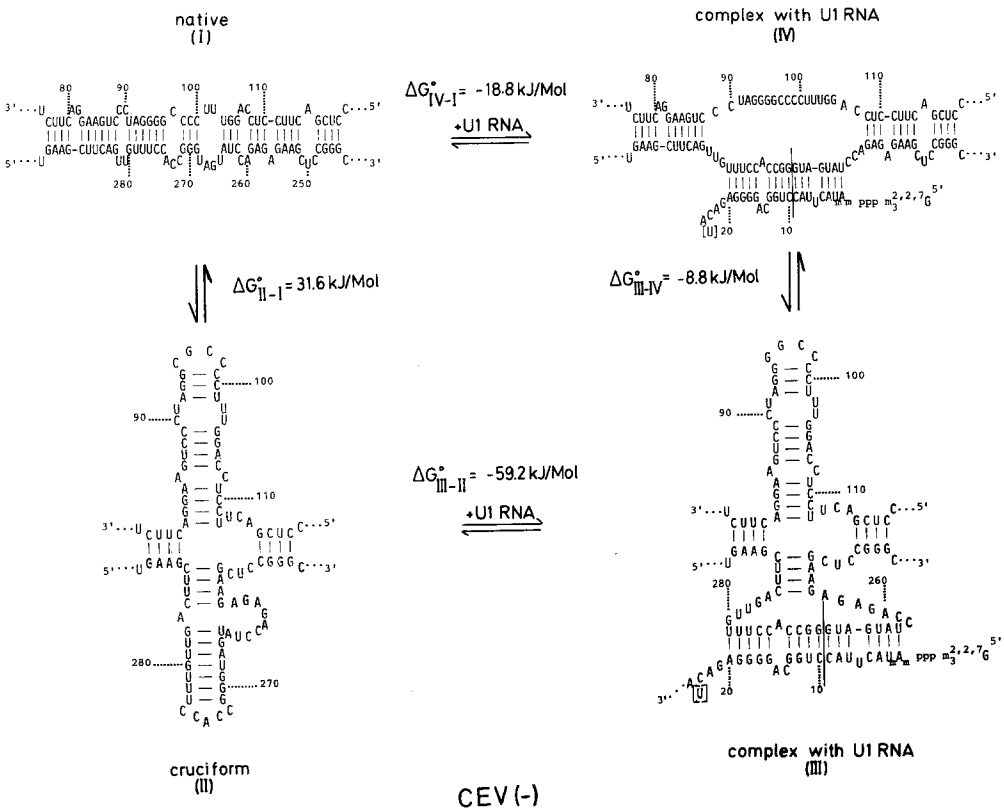

Fig. 13. Model of the splicing interference of viroids. In this example the complementary strand of CEV, denoted CEV(—), forms a complex with U1RNA. CEV(—) may be drawn in the extended or in the cruciform structure. The cruciform structure is only stable if complexed with U1RNA

intron-exon junctions may be formed as a prerequisite for the splicing process. It is known that the corresponding sequences in the mRNAs are conservative and the sequences of U1RNA from quite different organisms are nearly identical.

As mentioned above, much of the essential sequence in U1RNA agrees with the conservative sequence in the viroid. This agreement led to the following hypothesis (Diener 1981; Dickson 1981; Gross et al. 1982). Because the viroid

sequences which have been determined directly and their complementary copies, are present in the cell (Grill and Semancik 1978; Branch et al. 1981), two models of interaction may be discussed. In one mode the viroid could replace U1RNA and form basepairs with the intron of the heteronuclear RNA. In the other mode the complementary viroid would interact directly with U1RNA. The second mode is depicted in Fig. 13 (Randles et al. 1982). Only that part of the viroid is shown which can form the stable hairpin with its upper strand and in which the lower strand can interact with U1RNA. The cruciform structure (II) can be drawn theoretically with the upper and lower hairpin. Under the conditions of the experiments, where the existence of the upper hairpin was proven, the lower hairpin was not stable. From the $\Delta G°$-value in Fig. 13 it is evident that the cruciform structure (II) is highly unfavorable under native conditions. The situation changes drastically if the viroid-U1RNA-interaction is taken into account. U1RNA possibly interacts with the viroid in the extended (IV) or in the cruciform structure (III). If interacting with U1RNA, the cruciform structure is not at all disfavored but slightly more stable than the extended, as may be seen from the ΔG-values in Fig. 13. Consequently, U1RNA interaction may shift the structural equilibrium in the viroid by several orders of magnitude in favor of the cruciform. The ability of the viroid to form a stable hairpin in the upper strand makes the lower strand more easly available for U1RNA-interaction.

The hypothesis outlined above has two implications. First the interference of viroids with the splicing process could be the basis of viroid pathogenesis. Second because of the similarity of complementary viroids to introns, and because introns are also found in the form of circles, it is tempting to speculate that viroids may have been generated from escaped introns.

Acknowledgements. We thank Mr. M. Colpan for critically reading the manuscript and Mrs. H. Gruber and Mrs. B. Göbel for help in preparing the manuscript. The work was supported by grants from the Deutsche Forschungsgemeinschaft, Fonds der chemischen Industrie and the Alexander-von-Humboldt-Stiftung (J. W. R. during his stay in Düsseldorf).

References

Arnberg AC, van Ommen GJB, Grivell LA, van Bruggen EFJ, Borst P (1980) Some yeast mitochondrial RNAs are circular. Cell 19: 313–319

Borer PN, Dengler B, Tinoco J Jr, Uhlenbeck OC (1974) Stability of ribonucleic acid double stranded helices. J Mol Biol 86: 843–853

Branch AD, Robertson HD, Dickson E (1981) Longer-than-unit-length viroid minus strands are present in RNA from infected plants. Proc Natl Acad Sci USA 78: 6381–6385

Colpan M, Schumacher J, Brüggemann W, Sänger HL, Riesner D Large scale purification of viroid RNA using Cs_2SO_4-gradient centrifugation and HPLC. Submitted

De la Torre JG, Bloomfield VA (1981) Hydrodynamic properties of complex, rigid biological macromolecules: Theory and applications. Q. Rev Biophys 14: 81–139

Dickson E (1981) A model for the involvement of viroids in RNA splicing. Virology 115: 216–221

Diener TO (1971) Potato spindle tuber 'virus'. IV. A replicating low molecular weight RNA. Virology 45: 411–428

Diener TO (1979) Viroids: Structure and function. Science 205: 859–866

Diener TO (1981) Are viroids escaped introns? Proc Natl Acad Sci USA 78: 5014–5015
Diener TO, Lawson RH (1973) Chrysanthemum stunt: A viroid disease. Virology 51: 94–101
Gralla J, Crothers DM (1973a) Free energy of imperfect nucleic acid helices II. Small hairpin loops. J Mol Biol 73: 497–511
Gralla J, Crothers DM (1973b) Free energy of imperfect nucleic acid helices III. Small internal loops resulting from mismatches. J Mol Biol 78: 301–319
Grill LK, Semancik JS (1978) RNA sequences complementary to citrus exocortis viroid in nucleic acid preparations from infected Gynura aurantiaca. Proc Natl Acad Sci USA 75: 896–900
Gross HJ, Riesner D (1980) Viroids: A class of subviral pathogens. Angew Chem Int Ed Eng 19: 231–243; Angew Chem 92: 233–245
Gross HJ, Domdey H, Lossow Ch, Jank P, Raba M, Alberty H, Sänger HL (1978) Nucleotide sequence and secondary structure of potato spindle tuber viroid. Nature 273: 203–208
Gross HJ, Krupp G, Domdey H, Steger G, Riesner D, Sänger HL (1981) The structure of three plant viroids. Nucleic Acids Res (Symposium Series) 10: 91–98
Gross HJ, Krupp G, Domdey H, Raba M, Jank P, Lossow Ch, Alberty H, Ramm K, Sänger HL (1982) Nucleotide sequence and secondary structure of citrus exocortis and chrysanthemum stunt viroid. Eur J Biochem 121: 249–257
Haseloff J, Symons RH (1981) Chrysanthemum stunt viroid: Primary sequence and secondary structure. Nucleic Acids Res 9: 2741–2752
Haseloff J, Symons RH (1982) Comparative sequences and structure of viroid-like RNAs of two plants viruses. Nucleic Acids Res 10: 3681–3691
Haseloff J, Mohamed NA, Symons RH (1982) Viroid RNAs of cadang-cadang disease of coconuts. Nature 299: 316–321
Henco K, Sänger HL, Riesner D (1979) Fine structure melting of viroids as studied by kinetic methods. Nucleic Acids Res 6: 3041–3059
Henco K, Steger G, Riesner D (1980) Melting curves on less than 1 μg of nucleic acid. Anal Biochem 101: 225–229
Hollings M, Stone OM (1973) Some properties of chrysanthemum stunt, a virus with the characteristics of an uncoated ribonucleic acid. Ann Appl Biol 74: 333–348
Imperial JS, Rodriguez MJB, Randles JW (1981) Variation in the viroid-like RNA associated with cadang-cadang disease: Evidence for an increase in molecular weight with disease progress. J Gen Virol 56: 77–85
Kleinschmidt AK, Klotz G, Seliger H (1981) Viroid structure. Ann Rev Biophys Bioeng 10: 115–132
Kovacic RT, van Holde KE (1977) Sedimentation of homogeneous double-strand DNA molecules. Biochemistry 16: 1490–1498
Langowski J, Henco K, Riesner D, Sänger HL (1978) Common structural features of different viroids: Serial arrangement of double helical sections and internal loops. Nucleic Acids Res 5: 1589–1610
Lerner MR, Boyle JA, Mount SM, Wolin SL, Steitz JA (1980) Are snRNPs involved in splicing? Nature 283: 220–224
McClements W, Kaesberg P (1977) Size and secondary structure of potato spindle tuber viroid. Virology 76: 477–484
Ming-Ta Hsu, Coca-Prados M (1979) Electronmicroscopic evidence for the circular form of RNA in the cytoplasm of eukaryotic cells. Nature 280: 339–340
Mohamed NA, Imperial J, Haseloff J, Buenaflor G, Randles JW (1981) Variation in the viroid-like RNA associated with cadang-cadang disease of coconut. V. International Congress of Virology, Strasbourg 1981, abstract P 21/11
Owens RA, Smith DR, Diener TO (1978) Measurement of viroid sequence homology by hybridization with complementary DNA prepared in vitro. Virology 89: 388–394
Pörschke D, Uhlenbeck OC, Martin FH (1973) Thermodynamics and kinetics of the helix-coil transition of oligomers containing GC basepairs. Biopolymers 12: 1313–1335
Rackwitz HR, Rohde W, Sänger HL (1981) DNA-dependent RNA polymerase II of plant origin transcribes viroid RNA into full-length copies. Nature 291: 297–301
Randles JW (1975) Association of two ribonucleic acid species with cadang-cadang disease of coconut palm. Phytopathology 65: 163–167

Randles JW, Davies C, Hatta T, Gould AR, Francki RIB (1981) Studies on encapsidated viroid-like RNA I. Characterization of Velvet tobacco mottle virus. Virology 108: 111–122

Randles JW, Steger G, Riesner D (1982) Structural transitions in viroid-like RNAs associated with Cadang-cadang disease, Velvet tobacco mottle virus, and *Solanum nodiflorum* mottle virus. Nucleic Acids Res 10: 5569–5586

Riesner D, Römer R (1973) Thermodynamics and kinetics of conformational transitions in oligonucleotides and tRNA. In: Duchesne J (ed) Physico-chemical properties of nucleic acids, vol 2. Academic Press, London New York, pp 237–318

Riesner D, Henco K, Rokohl U, Klotz G, Kleinschmidt AK, Domdey H, Jank P, Gross HJ, Sänger HL (1979) Structure and structure formation of viroids. J Mol Biol 133: 85–115

Riesner D, Colpan M, Randles JW (1982a) A microcell for the temperature-jump technique. Anal Biochem 121: 186–189

Riesner D, Kaper JM, Randles JW (1982b) Stiffness of viroids and viroid-like RNA in solution. Nucleic Acids Res 10: 5587–5598

Romaine CP, Horst RK (1975) Suggested viroid etiology for chrysanthemum chlorotic mottle disease. Virology 64: 86–95

Rubin H, Kallenbach NR (1975) Conformational statistics of short RNA chains. J Chem Phys 62: 2766–2776

Sänger HL (1972) An infectious and replicating RNA of low molecular weight: The agent of the exocortis disease of citrus. Adv. Biosci 8: 103–116

Sänger HL (1980) Structure and possible functions of viroids. Ann NY Acad Sci 354: 251–278

Sänger HL, Klotz G, Riesner D, Gross HJ, Kleinschmidt AK (1976) Viroids are single-stranded covalently closed circular RNA molecules existing as highly base-paired rod-like structures. Proc Natl Acad Sci USA 73: 3852–3856

Sasaki M, Shikata E (1977) On some properties of hop stunt disease agent, a viroid. Proc Jpn Acad Ser B 53: 109–112

Scheffler JE, Elson EL, Baldwin RL (1970) Helix formation by d(TA)-Oligomers II. Analysis of the helix-coil transitions of linear and circular oligomers. J Mol Biol 48: 145–171

Semancik JS, Weathers LG (1972) Exocortis disease: Evidence for a new species of 'infectious' low molecular weight RNA in plants. Nature (New Biol) 237: 242–244

Singh RP, Clark MC (1971) Infectious low molecular weight ribonucleic acid from tomato. Biochem Biophys Res Commun 44: 1077–1083

Steger G, Gross HJ, Randles JW, Sänger HL, Riesner D (1983) Thermodynamic calculations on the stability and conformational transitions of viroids. (manuscript in preparation)

Symons RH (1981) Avocado sunblotch viroid: Primary sequence and proposed secondary structure. Nucleic Acids Res 9: 6527–6537

Thomas W, Mohamed NA (1979) Avocado sunblotch – A viroid disease? Aust Plant Pathol Soc Newslett 8: 1–3

Van Dorst HJM, Peters D (1974) Some biological observation on pale fruit, a viroid-incited disease of cucumber. Neth J Plant Pathol 870: 85–95

Visvader JE, Bould AR, Bruening GE, Symons RH (1982) Citrus exocortis viroid: Nucleotide sequence and secondary structure of an Australian isolate. FEBS Lett 137: 288–292

Wild U, Ramm K, Sänger HL, Riesner D (1980) Loops in viroids. Eur J Biochem 103: 227–235

Yamakawa H, Fujii M (1973) Translation friction coefficient of worm-like chains. Macromolecules 6: 407–415

Zelazny B, Randles JW, Boccardo G, Imperial JS (1982) The cadang-cadang disease of coconut palm. Scientia Filipinas (in press)

Received May 14, 1982/Accepted August 31, 1982